

A Novel DFT Spreading Technique for Reduction of Peak- to-Average Power Ratio (PAPR) in OFDM Systems

Soumik Basak, Koustav Sarkar, Deepak Kumar, Sudarshan Chakravorty

Abstract—The transmitted signal in an OFDM system can have high peak values due to the presence of many subcarriers. The high Peak-to-average Power Ratio (PAPR), as compared to a single carrier system in an OFDM system is detrimental for its proper operation. It decreases the signal-to- quantization noise ratio (SQNR) of the Analog-to-Digital and Digital-To-Analog converters. This degrades the efficiency of the power amplifiers in the transmitter. This paper aims to improve the PAPR in the uplink by DFT spreading so as to preserve the limited battery power in a mobile terminal.

IndexTerms— DFT spreading, OFDM, Peak-to-Average Power Ratio, SQNR.

I. INTRODUCTION

Non linear distortion from the output of the high power amplifier stages of the transmitter of the OFDM system is a problem which severely limits its operational capability. This results in severe signal distortion in their outputs on account of the saturation caused by the input much larger than the nominal value.

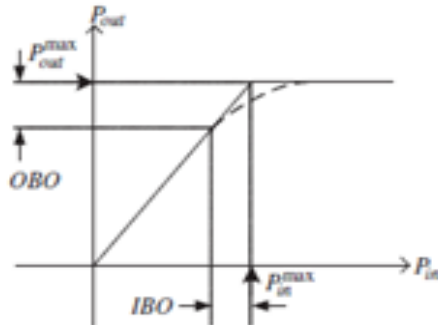


Fig 1 Input-output characteristic of an HPA.

Fig1 shows the input-output characteristics of the high power amplifier (HPA) in terms of the input power P_{in} and the output power P_{out} . Due to the above mention saturation characteristic of the amplifier, the maximum possible output is limited by $(P_{out})_{max}$; when the corresponding input power is $(P_{in})_{max}$. Accordingly, as given in the Fig. 1, the input power must be backed off, so as to operate in the linear region. Therefore, the non-linear region can be described by IBO(Input- Back- Off) and OBO(Output-Back-Off) in [1].

Manuscript received on May, 2013.

SoumikBasak, ECE department, MCKV Institute of Engineering Howrah, India.

KoustavSarkar, ECE department, MCKV Institute of Engineering Howrah, India.

Deepak kumar, ECE department, MCKV institute of Engineering, Howrah, India.

SudarshanChakravorty, ECE department, MCKV Institute of Engineering, Howrah, India.

$$IBO=10\log_{10}(P_{in})_{max}/P_{in}, \quad OBO=10\log_{10}(P_{out})_{max}/P_{out}$$

This PAPR causes out-of-band radiation that affects signals in adjacent bands and offset on the received signal[2]. This paper aims to reduce the PAPR through DFT spreading. The advantage of this system is that the transmit signal will have the same PAPR as that of a signal-carrier system.

II. DFT SPREADING

Before going into the DFT spreading technique, let us consider OFDMA[3]. Among the multiple access techniques associated with OFDM, OFDMA is one of the most useful approaches in the mobile cellular system. This is possible because in the condition of different signal to interference and noise ratios(SINRs) in different cells, users are allowed to select their own subset of subcarriers with better channel conditions, as given in Figure2, the DFT is taken as the same .

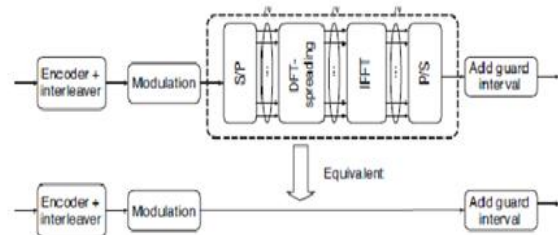


Fig 2 Equivalence of OFDMA system with DFT-spreading code to a single-carrier system.

As given in Fig2, the DFT is taken as the same size as IFFT of an OFDMA system, which is used as a spreading code. Under this circumstances, OFDMA becomes equivalent to the Single Carrier FDMA[SC-FDMA] system, because the DFT and IDFT operations virtually cancel each other[4].in this case, the transmit signal will have the same PAPR as in a single-carrier system.

In OFDMA systems, subcarriers are partitioned and assigned to multiple mobile terminals (users). Unlike the downlink transmission, each terminal in uplink uses a subset of subcarriers to transmit its own data. The rest of the subcarriers, not used for its own data transmission, will be filled with zeros. Here, it will be assumed that the number of subcarriers allocated to each user is M . In the DFT-spreading technique, M -point DFT is used for spreading, and the output of DFT is assigned to the subcarriers of IFFT. The effect of PAPR reduction depends on the way of assigning the subcarriers to each terminal. As depicted in Figure 3, there are two different approaches of assigning subcarriers among users: DFDMA (Distributed FDMA) and LFDMA (Localized FDMA).

Here, DFDMA distributes M DFT outputs over the entire band (of total N subcarriers) with zeros filled in (N-M) unused subcarriers, whereas LFDMA allocates DFT outputs to M consecutive subcarriers in N subcarriers. When DFDMA distributes DFT outputs with equidistance N/M = S, it is referred to as IFDMA (Interleaved FDMA) where S is called the bandwidth spreading factor.

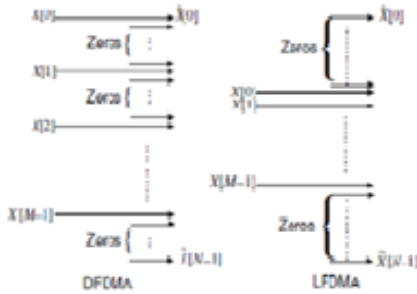


Fig 3 Subcarrier mapping for uplink in OFDMA systems: DFDMA and LFDMA.

Fig 4 illustrates the subcarriers allocated in the DFDMA and IFDMA with M = 4, S = 3, and N = 12. Furthermore, Figure 5 shows the examples of DFT spreading in DFDMA, LFDMA, and IFDMA with N = 12, M = 4, and S = 3. It illustrates a subcarrier mapping relationship between 4-point DFT and 12-point IDFT

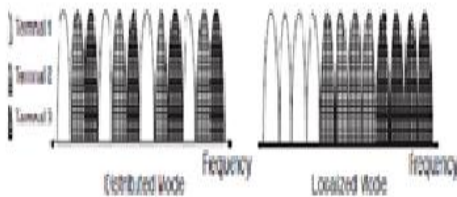


Fig 4 Examples of subcarrier assignment to multiplexers three users with N = 12, M = 4, and S = 3.

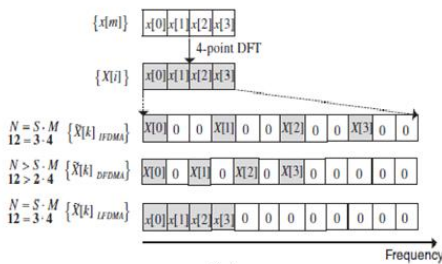


Fig 5 Examples of DFT spreading for IFDMA, DFDMA and LFDMA: three users with N = 12, M = 4, and S = 3.

Fig. 6 shows a block diagram of the uplink transmitter with the DFT-spreading technique that employs IFDMA. Here, the input data x[m] is DFT-spread to generate X[i] and then, allocated as:

$$\hat{X}[k] = X\left[\frac{k}{S}\right], K = S \cdot m_1, m_1 = 0, 1, 2, \dots, M-1 \neq 0, \text{otherwise} \quad (1)$$

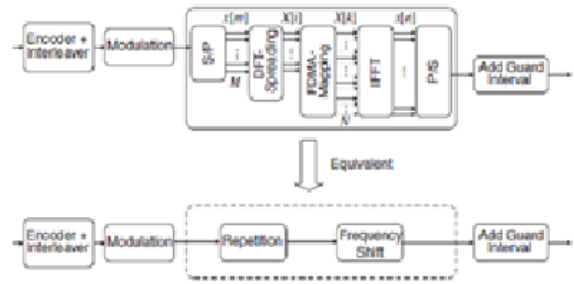


Fig 6 Uplink transmitter with DFT-spreading technique of IFDMA.

The IDFT output sequence x[n] with n = M · s + m for s = 0, 1, 2, ..., S-1 and m = 0, 1, 2, ..., M-1 can be expressed as,

$$\begin{aligned} \hat{X}[n] &= \frac{1}{N} \sum_{k=0}^{N-1} \hat{x}(k) e^{j2\pi \frac{n \cdot k}{N}} \\ &= \left(\frac{1}{S}\right) \cdot \left(\frac{1}{M}\right) \sum_{m_1=0}^{M-1} x[m_1] \cdot e^{j2\pi \frac{n}{M} m_1} \\ &= \left(\frac{1}{S}\right) \cdot \left(\frac{1}{M}\right) \sum_{m_1=0}^{M-1} x[m_1] \cdot e^{j2\pi \left(\frac{M_s + m_s}{M}\right) m_1} \quad (2) = \left(\frac{1}{S}\right) \cdot \left(\frac{1}{M}\right) \sum_{m_1=0}^{M-1} x[m_1] \cdot e^{j2\pi \left(\frac{n}{M}\right) m_1} \\ &= \frac{1}{S} \cdot x[m] \end{aligned}$$

This is nothing but a replica of the original signal x[m] scaled by 1/s in the time domain [5]. In the IFDMA where the subcarrier mapping starts with the rth subcarrier (r = 0; 1; 2; ... ; S-1), the DFT-spread symbol can be expressed as $X^{\wedge}(K) = \{ X[(K-r)/S], K = S \cdot m_1 + r, m_1 = 0, 1, 2, \dots, M-1 \neq 0 \text{ otherwise} \}$ (3)

Then, the corresponding IDFT output sequence, {x[^][n]} is given

$$\begin{aligned} \hat{X}[n] &= \hat{X}[m_s + m] \\ \hat{X}[n] &= \left(\frac{1}{N}\right) \sum_{k=0}^{N-1} \hat{X}[k] \cdot e^{j2\pi \left(\frac{n}{N}\right) k} \\ &= \left(\frac{1}{S}\right) \cdot \left(\frac{1}{M}\right) \sum_{m_1=0}^{M-1} x[m_1] e^{j2\pi \left(\frac{n}{M}\right) m_1 + \frac{n}{N} r} \\ &= \left(\frac{1}{S}\right) \cdot \left(\frac{1}{N}\right) \cdot \sum_{m_1=0}^{M-1} x[m_1] \cdot e^{j2\pi \left(\frac{m_s + m}{M}\right) m_1} \cdot e^{j2\pi \left(\frac{n}{N}\right) r} \\ &= \left(\frac{1}{S}\right) \cdot \left(\frac{1}{N}\right) \cdot \sum_{m_1=0}^{M-1} x[m_1] \cdot e^{j2\pi \left(\frac{n}{M}\right) m_1} \cdot e^{j2\pi \left(\frac{n}{N}\right) r} \\ &= \frac{1}{S} \cdot e^{j2\pi \left(\frac{n}{N}\right) r} \cdot x[m] \quad (4) \end{aligned}$$

If we compared with (2), one can see that the frequency shift of subcarrier allocation starting point by r subcarriers results in the phase rotation of e^{j2πnr/N} in IFDMA.



In the DFT-spreading scheme for LFDMA, the IFFT input signal $x^{\wedge}[k]$ at the transmitter can be expressed as $\hat{X}[k]=\{x[k], k=0, 1, 2 \dots M-1 = 0, k=M; M+1 \dots N-1\}$ (5)

The IFFT output sequence $x[n]$ with $n = S \cdot m + s$ for $s= 0; 1; 2; \dots; S-1$ can be expressed as follows

$$\hat{X}[m] = \hat{X}[s_m + s] = \frac{1}{N} \sum_{k=0}^{N-1} \hat{X}[k] e^{j \cdot 2\pi \cdot (\frac{n}{N}) \cdot k}$$

$$= \left(\frac{1}{S}\right) \cdot \left(\frac{1}{M}\right) \sum_{k=0}^{M-1} x(k) e^{j \cdot 2\pi \cdot (\frac{s_m + s}{s \cdot M}) \cdot k} \quad (6)$$

If we consider, $s=0$, then Equation (6) becomes

$$\hat{X}[n] = x[s_m] = \left(\frac{1}{S}\right) \cdot \left(\frac{1}{M}\right) \sum_{k=0}^{M-1} x[k] e^{j \cdot 2\pi \cdot (\frac{s_m}{s \cdot M}) \cdot k}$$

$$= \left(\frac{1}{S}\right) \cdot \left(\frac{1}{M}\right) \cdot \sum_{k=0}^{M-1} x[k] \cdot e^{j \cdot 2\pi \cdot (\frac{m}{N}) \cdot k}$$

$$= \left(\frac{1}{S}\right) \cdot (x[m]) \quad (7)$$

For $s \neq 0, x[k] = \sum_{p=0}^{M-1} x[p] \cdot e^{j \cdot 2\pi \cdot \frac{k}{N} \cdot p}$ such that (6) becomes

$$\hat{X}[n] = \hat{X}[s_m + s]$$

$$= \left(\frac{1}{S}\right) \cdot (1 - e^{j \cdot 2\pi \cdot \frac{s}{S}}) \cdot \left(\frac{1}{M}\right) \sum_{p=0}^{M-1} \frac{x[p]}{1 - e^{j \cdot 2\pi \cdot (\frac{sm-p}{M} + \frac{s}{s \cdot M})}}$$

$$= \frac{1}{S} \cdot e^{j \pi \cdot \frac{(M-1)s - sM}{s \cdot M}} \cdot \sum_{p=0}^{M-1} \frac{\sin \pi \cdot (\frac{s}{S})}{M \sin \left(\pi \cdot \left(\frac{sm+s}{sM} - \pi \cdot \frac{p}{M} \right) \right)} \cdot (e^{j \pi \cdot \frac{p}{M}} \cdot x[p]) \quad (8)$$

From (7) and (8), it can be seen that the time domain LFDMA signal becomes the $1/s$ scaled copies of the input sequence in the time domain. The in-between values can be obtained by summing all the input sequences with the complex weighted factor $c(m, s, p)$.

III. RESULTS AND DISCUSSIONS

Fig.6 shows a comparison of PAPR performances when the DFT-spreading technique is applied to the IFDMA, LFDMA, and OFDMA. Here, QPSK, 16-QAM, and 64-QAM are used for an SC-FDMA system with $N = 256, M = 64,$ and $S = 4$. It can be seen from Fig 7 that the PAPR performance of the DFT-spreading technique varies depending on the subcarrier allocation method. In the case of 16-QAM, the values of PAPRs with IFDMA, LFDMA, and DFDMA for CCDF of 1% are 3.5dB, 8.3dB, and 10.8dB, respectively. It implies that the PAPRs of IFDMA and LFDMA are lower by 7.3dB and 3.2dB, respectively, than that of OFDMA with no DFT spreading.

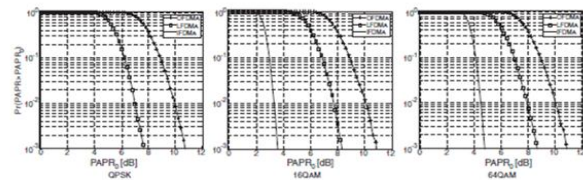


Fig 6 PAPR performances of DFT-spreading technique for IFDMA, LFDMA, and OFDMA.

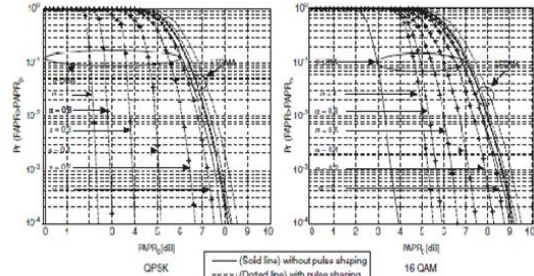
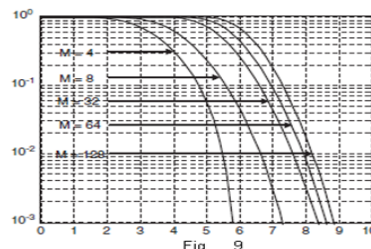


Fig 7 PAPR performances of DFT-spreading technique with pulse shaping.

Considering the effect of pulse shaping on the PAPR performance of DFT-spreading technique, Fig 8 shows the PAPR performance of DFT-spreading technique with IFDMA and LFDMA, varying with the roll-off factor α of the RC (Raised-Cosine) filter for pulse shaping with IFFT. It can be seen from this figure that the PAPR performance of IFDMA can be significantly improved by increasing the roll-off factor from $\alpha = 0$ to 1. This is instark contrast with LFDMA which is not so much affected by pulse shaping. The result clearly implies that IFDMA will have a trade-off between excess bandwidth and PAPR performance since excess bandwidth increases as the roll-off factor increases from 0 to 1. The above results here have been obtained with the simulation parameters of $N = 256, M = 64, S = 4$ (spreading factor), and $Nos = 8$ (oversampling factor for pulse shaping) for both QPSK and 16-aryQAM.

To analyze the performance of the PAPR of DFT-spreading technique is affected by the no of subcarriers, M , that are allocated to each user; fig9 shows the PAPR performance of DFT spreading technique for LFDMA. Here the roll off factor is chosen as $\alpha=.4$ as it is clearly seen that the PAPR performance degrades as M is being increased from 4 to 128. 64-ary QAM is used for the single carrier-FDMA (SC-FDMA) with a 256 point FFT ($N=256$).



PAPR performance of DFT-spreading technique when M varies.

IV. CONCLUSION

From above, it can be concluded that the SC-FDMA systems with IFDMA and LFDMA have better PAPR performances, as compared to OFDMA systems.

This unique feature of SC-FDMA has been adopted for uplink transmission in 3GPPLTE, which is been, selected as one of the radio interface technologies for IMT-Advanced standards. LFDMA is preferred to IFDMA in spite of the latter having lower PAPR as compared to the former, because of the fact that the allocation of the subcarriers with an equidistance of the entire band is not easy to implement. This is because of the additional requirements of guard bands and pilots.

REFERENCES

- [1] Litsyn.s(2007) Peak Power Control in Multicarrier Communications, Cambridge University Press.
- [2] Han S.H. and Lee J.H.(2005)"An overview of peak-to-average power ratio reduction techniques for multicarrier transmission," IEEE Trans in Wireless Communication, 12(2),56-65.
- [3] Jeon W.G., Chang K.H., and Cho Y.S. (1997) "An adaptive data predistorter for compensation of nonlinear distortion in OFDM system", IEEE Trans in comm..., 45(10), 1167-1171.
- [4] Galda, D and Rohling,H.(2002)"A low complexity transmitter structure for OFDM-FDMA uplink system",IEEE VTC'02, Vol.4,pp 1737-1741.
- [5] Myung, H.G., Lin,J, and goodman D.J. "peak-to-average power ratio of Single Carrierfdma signals with pulse shaping", PIMRC'06,pp1-5.



Mr. Soumik Basak is final year M.Tech student in ECE dept. of MCKV Institute of Engineering. His current areas of interest are OFDM and Mobile Communication.



Mr. Koustav Sarkar is final year M.Tech student in ECE dept. of MCKV Institute of Engineering. His current areas of interest are Mobile Communication and Micro-strip Patch Antenna.



Mr. Deepak Kumar is final year B.Tech student in ECE dept.of MCKV Institute of Engineering. His current areas of interest are OFDM,Mobile Communication and RADAR.



Mr. Sudarshan Chakravorty is an associate professor in ECE dept. of MCKV Institute of Engineering. He has around 30 years' of experience in teaching and industry. He has published more than twenty research papers in international journals. His current areas of interest are Radar Application and Mobile Communication. Currently he is doing his PhD. work in the area of Thermal Modeling of IMPATT Diode.